Stem Cell Research (2014) 12, 241–249

Available online at www.sciencedirect.com

ScienceDirect

www.elsevier.com/locate/scr

SHORT REPORT

Electrophysiological properties of neurosensory progenitors derived from human embryonic stem cells

Karina Needham[a,b,*], Tomoko Hyakumura[a,1], Niliksha Gunewardene[a,1], Mirella Dottori[c], Bryony A. Nayagam[a,d,e,**]

[a] *Department of Otolaryngology, University of Melbourne, Royal Victorian Eye and Ear Hospital, Level 2, 32 Gisborne Street, East Melbourne, VIC 3002, Australia*
[b] *Department of Medicine, St Vincent's Hospital, University of Melbourne, Level 4, Clinical Sciences Building, 29 Regent Street, Fitzroy, VIC 3065, Australia*
[c] *Centre for Neural Engineering, NICTA, University of Melbourne, 203 Bouverie Street, Parkville, VIC 3010, Australia*
[d] *Department of Audiology and Speech Pathology, University of Melbourne, 550 Swanston Street, Parkville, VIC 3010, Australia*
[e] *Bionics Institute, 384–388 Albert Street, East Melbourne, VIC 3002, Australia*

Received 6 August 2013; received in revised form 30 October 2013; accepted 30 October 2013
Available online 7 November 2013

Abstract In severe cases of sensorineural hearing loss where the numbers of auditory neurons are significantly depleted, stem cell-derived neurons may provide a potential source of replacement cells. The success of such a therapy relies upon producing a population of functional neurons from stem cells, to enable precise encoding of sound information to the

Abbreviations: 4-AP, 4-aminopyridine; AN, auditory neuron; AP, action potential; AP_{Max}, maximum number of action potentials; BDNF, brain derived neurotrophic factor; bFGF, basic fibroblast growth factor; cDNA, complementary deoxyribonucleic acid; DIV, days *in vitro*; EGF, epidermal growth factor; HCN, hyperpolarization-activated cyclic nucleotide-gated channels; hESC, human embryonic stem cell; HFFs, human foreskin fibroblast feeders; I_h, hyperpolarization-activated current; I_K, potassium current; I_{Na}, sodium current; K, slope factor; NBM, Neurobasal media; NFM, neurofilament; NS, neurosphere; NT3, neurotrophin 3; NTs, neurotrophins; pps, pulses per second; qRT-PCR, quantitative real time polymerase chain reaction; R_{IN}, input resistance; R_S, series resistance; RMP, resting membrane potential; RNA, ribonucleic acid; SEM, standard error of the mean; TEA, tetraethylammonium; TTX, tetrodotoxin; V_h, half-activation voltage; Y27, small peptide Y27632; ZD7288, 4-ethylphenylamino-1,2-dimethyl-6-methylaminopyrimidinium chloride

* Correspondence to: K. Needham, Department of Otolaryngology, University of Melbourne, Royal Victorian Eye and Ear Hospital, Level 2, 32 Gisborne Street, East Melbourne, VIC 3002, Australia. Fax:+61 3 9663 1958.
** Correspondence to: B. Nayagam, Department of Audiology and Speech Pathology, University of Melbourne, 550 Swanston Street, Parkville, VIC 3010, Australia. Fax: +61 3 9347 9736.
E-mail addresses: k.needham@unimelb.edu.au (K. Needham), t.hyakumura@pgrad.unimelb.edu.au (T. Hyakumura), gunan@unimelb.edu.au (N. Gunewardene), mdottori@unimelb.edu.au (M. Dottori), b.nayagam@unimelb.edu.au (B.A. Nayagam).
[1] These authors contributed equally to this study.

http://dx.doi.org/10.1016/j.scr.2013.10.011

brainstem. Using our established differentiation assay to produce sensory neurons from human stem cells, patch-clamp recordings indicated that all neurons examined generated action potentials and displayed both transient sodium and sustained potassium currents. Stem cell-derived neurons reliably entrained to stimuli up to 20 pulses per second (pps), with 50% entrainment at 50 pps. A comparison with cultured primary auditory neurons indicated similar firing precision during low-frequency stimuli, but significant differences after 50 pps due to differences in action potential latency and width. The firing properties of stem cell-derived neurons were also considered relative to time in culture (31–56 days) and revealed no change in resting membrane potential, threshold or firing latency over time. Thus, while stem cell-derived neurons did not entrain to high frequency stimulation as effectively as mammalian auditory neurons, their electrical phenotype was stable in culture and consistent with that reported for embryonic auditory neurons.

Introduction

Sensorineural hearing loss occurs when the delicate sensory hair cells of the inner ear are injured by factors such as loud noise, trauma, and exposure to ototoxic compounds or simply ageing. Currently, the principal treatment for sensorineural hearing loss is a cochlear implant. This device reinstates the transmission of sound information to the central auditory pathway by providing direct electrical stimulation to the primary auditory neurons (in the absence of hair cells; Seligman and Shepherd, 2004). This neural population provides the critical link between the peripheral cochlea and the central auditory system, and auditory neurons are capable of responding to high stimulation rates with temporal acuity (Kiang et al., 1965; Javel and Viemeister, 2000). Importantly, while the cochlear implant relies upon a functional population of primary auditory neurons to convey auditory input to higher neural centers, these auditory neurons themselves are often vulnerable to degeneration after hearing loss, or may even be the site of primary damage. An extensive loss of primary auditory neurons is assumed to significantly reduce the effectiveness of a cochlear implant.

Stem cells offer an opportunity to restore auditory function by replacing lost auditory neurons in cases of severe depletion. A number of studies have now demonstrated the potential of stem cells to differentiate into appropriate neurosensory progenitors, including those of human origin (Shi et al., 2007; Chen et al., 2009, 2012; Nayagam et al., 2013). The expression of key developmental markers in the differentiation of human stem cells toward an auditory neural lineage has recently been documented (Chen et al., 2012; and reviewed by Gunewardene et al., 2012) and includes the expression of key proteins and transcription factors Sox 2, Pax2/8, FoxG1, Six1, Nestin and Brn3a (Chen et al., 2012), Brn3a, GATA3 and peripherin (Shi et al., 2007), Pax2, Brn3a, peripherin, and neurofilament (Nayagam et al., 2013) and *NeuroD1,* Brn3a, GATA3, Islet1, peripherin, and neurofilament (Gunewardene et al., 2013).

The method used to generate sensory neurons in the present study is based on previously published protocols from our laboratories for deriving neural crest progenitors (Holt et al., 2006; Denham and Dottori, 2011; Liu et al., 2011; Nayagam et al., 2013). Recent literature supports the use of neural crest progenitors in a cell replacement therapy for deafness, given the molecular similarity of this population to placode-derived sensory neurons (Huisman and Rivolta, 2012; Nayagam et al., 2013). In addition, we have recently demonstrated that neurons derived from this induction protocol express key auditory neural proteins including *NeuroD1*, Brn3a, GATA3, Islet1 and neurofilament (Fig. 1; Gunewardene et al., 2013) and are capable of making synapses on developing mammalian hair cells *in vitro* (Nayagam et al., 2013). Given that neural crest progenitors can also be readily obtained from adults (Yang and Xu, 2013), they have the potential to facilitate the development of patient-matched cell transplants in the future (Huisman and Rivolta, 2012; Yang and Xu, 2013).

An important challenge to overcome in developing a cell replacement therapy for hearing loss is the development of a functionally stable stem cell-derived neural population (Needham et al., 2013). This entails both the development of electrically active neurons and their functional integration including formation of synapses with target neurons in the cochlear nucleus. We and others have previously shown that human stem cell-derived neurons can fire action potentials, and possess the core currents and channel families necessary for this task (Chen et al., 2009; Nayagam et al., 2013). Among these are the inward Na^+ currents (I_{Na}) and sustained outward K^+ currents (I_K). These are arguably the most basic currents necessary to instigate action potentials, and therefore communicate meaningful signals to their target/s. The next milestone in our experimentation is to develop neurons with an electrical phenotype capable of processing information in a similar manner to the primary auditory neurons. Most notably, the glutamatergic primary auditory neurons possess a large complement of ion channels that enable them to respond to complex signals with temporal precision (reviewed Needham et al., 2013). A key feature of this neural phenotype is the ability to reliably follow high frequency stimulation since this is a hallmark of acoustic stimuli, as well as the electrically encoded input from a cochlear implant. Interestingly, little is known about the definitive firing rates of auditory neurons in response to electrical stimulation in humans. However, what is clear from clinical studies, is that pitch discrimination deteriorates as stimulation levels approach 300 pulses per second (Shannon, 1983; Zeng, 2002; Vandali et al., 2013). Thus, based upon these data, it seems reasonable to expect that replacement neurons be capable of firing at similar rates to endogenous auditory neurons as a reduction in firing entrainment would likely affect the amount of information encoded in the signal relayed to the brain, and therefore the accurate perception of sound.

Here we examine the electrical profile of human embryonic stem cell (hESC) derived neurosensory progenitors over time *in vitro*, and compare their responses to high frequency stimulation with that of the primary auditory neuron population.

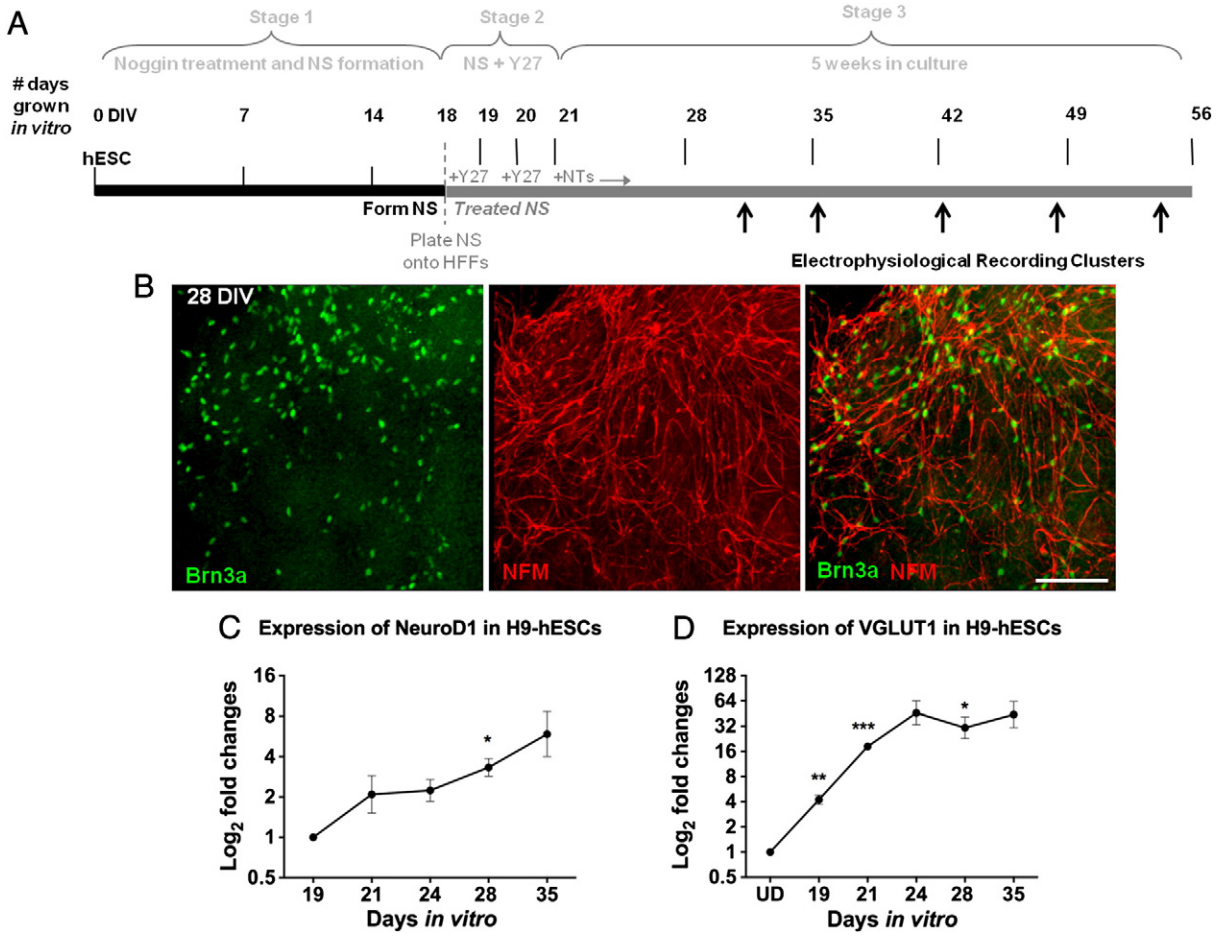

Figure 1 Timeline of hESC differentiation, electrophysiological recordings and neurosensory protein expression *in vitro*. (A) Neurosphere (NS) formation (stage 1) was followed by treatment with ROCK/Rho kinase inhibitor Y27632 (Y27; stage 2) and neurotrophins (NTs; stage 3). Electrophysiological recordings were made between 31 and 56 days *in vitro* (DIV); recording clusters denoted by arrows. (B) Immunocytochemical assessment of cells at 28 DIV revealed expression of key markers of auditory neural lineage, Brn3a and neurofilament (NFM). Scale bar = 100 μm (relative to all images). (C–D) Expression of *NeuroD1* (C) and VGLUT1 (D) at 19, 21, 24, 28 and 35 DIV as measured by qRT-PCR. Results presented as fold changes relative to the endogenous control, ß-actin. Significance: $^{*}p < 0.05$; $^{**}p < 0.01$; $^{***}p < 0.001$. DIV — days *in vitro*; hESC — human embryonic stem cell; HFFs — human foreskin fibroblast feeders; UD — undifferentiated.

Materials and methods

Stem cell culture

The following procedures are based on protocols described previously by Dottori and Pera (2008), Hotta et al. (2009), and Nayagam et al. (2013). The H9 human embryonic stem cell line (WA-09, WiCell) was cultured in 20% serum-containing medium on mitomycin-C-treated human foreskin fibroblast feeders (HFFs) and passaged weekly by mechanical dissociation. For neural induction, mechanically dissociated hESCs were placed on a fresh HFF feeder layer in organ culture dishes with Neurobasal media (NBM) supplemented with 500 ng/ml recombinant noggin (R&D Systems). Neurobasal media contained Neurobasal A medium supplemented with 1% N2, 2% B27, 2 mM L-glutamine and 0.5% penicillin/streptomycin (all sourced from Invitrogen). Cells were cultured for 14 days without passaging, and the media replaced every second day. To make neurospheres, fragments of noggin-treated colonies were mechanically dissected and transferred to individual wells of a low-attachment 96-well plate in NBM supplemented with epidermal growth factor (EGF) and basic fibroblast growth factor (bFGF) at 20 ng/ml each (Peprotech). After 4 days, neurospheres were plated onto HFF feeders grown on gelatin-coated glass coverslips (HFF density of 4.7×10^4 cells/coverslip) and cultured in NBM supplemented with EGF and bFGF (at 20 ng/ml each) for the first 24 h, then replaced with media containing EGF, bFGF and 25 μM Y27632 (Sigma Aldrich) for a further 48 h. Following Y27632 treatment, cultures were maintained at 37 °C (10% CO_2) in NBM supplemented with brain derived neurotrophic factor (BDNF) and neurotrophin 3 (NT3) at 10 ng/ml each (Chemicon) until required for electrophysiological recordings. Media was replaced every 2–3 days. The timeline of neural induction and electrophysiological recordings is illustrated in Fig. 1.

Quantitative real time polymerase chain reaction (qRT-PCR)

For qRT-PCR, hESCs were grown as described earlier with the exception that BDNF and NT3 were not added after 24 days *in vitro* (24 DIV). Cells were collected at five time points: 19, 21, 24, 28 and 35 DIV. RNA was extracted from samples using the SV Total RNA Isolation Kit (Promega Corporations) according to the manufacturer's instructions and quantified using a NanoDrop spectrophotometer (Thermoscientific). Equal amounts of total RNA (60 ng) per sample were reverse transcribed using the High Capacity RNA-to-cDNA kit (Life Technologies). The cDNA products were transferred into the qRT-PCR reaction using TaqMan gene expression master mix (Life technologies). Commercially available probes obtained from Life Technologies included *NeuroD1* (Hs01922995_s1: FAM dye), SLC17A7 (VGLUT1; Hs00220404_m1: FAM dye), and ß-actin as the housekeeper reference gene (4326315E: VIC dye, primer limited). Standard curves were generated for the probes by a 1:10 serial dilution of control cDNA sample and the reaction efficiencies were >95% for both probes. The qRT-PCR reactions were run in duplex with both the gene of interest probe and the housekeeping probe present. Negative controls included a no template control (water only) and a reverse transcriptase negative sample (without cDNA). qRT-PCR reactions were run using a RotorGene Q instrument (Qiagen, Hilden, Germany) and the Rotor-gene 6000 software (Version 1.7, Corbitt Research) was used to analyze the results. The $2^{-\Delta\Delta Ct}$ delta–delta analysis algorithm was used to determine the relative quantification of each sample at the time points analyzed (Livak and Schmittgen, 2001). The threshold values generated from each probe's standard curves were used to determine the CT values of the experimental samples. The expression levels of the experimental samples were measured in triplicate and normalized against the endogenous control, ß-actin, to obtain the ΔCt value. The ΔCt values were standardized against the calibrator's ΔCt (VGLUT1-undifferentiated stem cells; NeuroD1-19 DIV stem cells) to determine the ΔΔCt value. The relative quantification was then calculated as $2^{-\Delta\Delta Ct}$. Statistical analyses of the qRT-PCR data were performed using the GraphPad Prism. The relative quantification data were analyzed using a two-tailed Student's *t*-test, with assumed equal variance for comparison between the fold changes of the undifferentiated cells to differentiating cells at each time point noted ($n = 3$, per time point). Values of $p < 0.05$ were considered statistically significant. Data are presented as the mean ± standard error of the mean (SEM).

Immunocytochemistry

Stem cell cultures were fixed after 28 DIV, in a solution of 4% paraformaldehyde for 10 min. Cells were then rinsed three times for 10 min in phosphate buffered saline and immunostained for the neurosensory markers Brn3a (Millipore MAB1585; 1:1000) and Neurofilament medium subunit (NFM; Millipore AB5735; 1:1000), using identical methods to those previously described (Nayagam et al., 2013). Alexafluor secondary antibodies (Molecular Probes) were applied at a concentration of 1:500 and preparations mounted in ProLong Gold (Molecular Probes).

Auditory neuron culture

As described in detail previously (Needham et al., 2012; Brown et al., 2013), cultures of auditory neurons were prepared from postnatal day four to seven (P4–P7) Wistar rat pups. Dissociated cells were resuspended in NBM then plated onto circular glass coverslips (10 mm diameter; Menzel-Glaser) pre-coated for 1 day with poly-ornithine (500 μg/ml; Sigma) and mouse laminin (0.01 mg/ml; Invitrogen). Cultures were maintained at 37 °C (10% CO_2) for up to 48 h in NBM supplemented with BDNF and NT3 (media replenished daily). Primary auditory neurons were visually identified as round, phase-bright cells with ~15–20 μm soma diameter and a prominent eccentric nucleus (Needham et al., 2012).

Electrophysiology

Coverslips were transferred to a recording chamber fitted to an AxioExaminer D1 microscope (Carl Zeiss) for electrophysiological recordings. As previously detailed (Needham et al., 2012; Nayagam et al., 2013), cells were superfused at 1–2 ml/min with solution of the following composition (in mM): 137 NaCl, 5 KCl, 10 HEPES, 1 $MgCl_2$, 2 $CaCl_2$, 10 glucose (pH 7.35; 300–305 mOsmol/kg). Neurons were visually identified by a round-to-oval soma (diameter of ~10 μm) and patent bipolar processes. Whole-cell patch clamp recordings were made at room temperature using borosilicate microelectrodes (2–6 MΩ; 1.0 mm O.D.; 0.58 mm I.D., Sutter) filled with an internal solution containing (in mM): 115 K-gluconate, 10 HEPES, 7 KCl, 0.05 EGTA, 2 Na_2ATP, 2 MgATP, 0.5 Na_2GTP (pH 7.3; 290–295 mOsmol/kg). All chemicals were purchased from Sigma-Aldrich (Sydney, Australia) unless otherwise indicated.

Signals were recorded with a MultiClamp 700B amplifier (Molecular Devices), data acquisition system (Digidata 1440A, Molecular Devices), and AxoGraph X analysis software (AxoGraph Scientific). Records were digitized at 50 kHz and filtered at 10 kHz. Series resistance (R_S) was monitored in response to a 10 mV voltage step (mean 16 ± 0.6 MΩ; cells with R_S greater than 30 MΩ were excluded). R_S was routinely compensated online (up to 70%). No corrections were made for voltage errors for uncompensated R_S. In current clamp, pipette capacitance neutralization was applied and bridge balance utilized to compensate errors due to R_S. All recordings were made from a holding potential of −73 mV, and corrections for liquid junction potential (12.8 mV; JPCalcW, Prof P H Barry, Sydney) were made offline.

The normalized current–voltage relationship for instantaneous tail currents was fitted with the following Boltzmann equation $I - I_{min} / I_{max} - I_{min} = (1 + \exp((V - V_h) / K))^{-1}$, where V is the membrane potential, V_h the half-activation voltage, and K the slope factor. Statistical significance was determined by Student's *t*-tests, or ANOVA with Tukey method for pairwise comparisons (MiniTab 16); data were considered significant where $p < 0.05$. Results are presented as mean values ± SEM; n denotes the number of cells in which measurements were made.

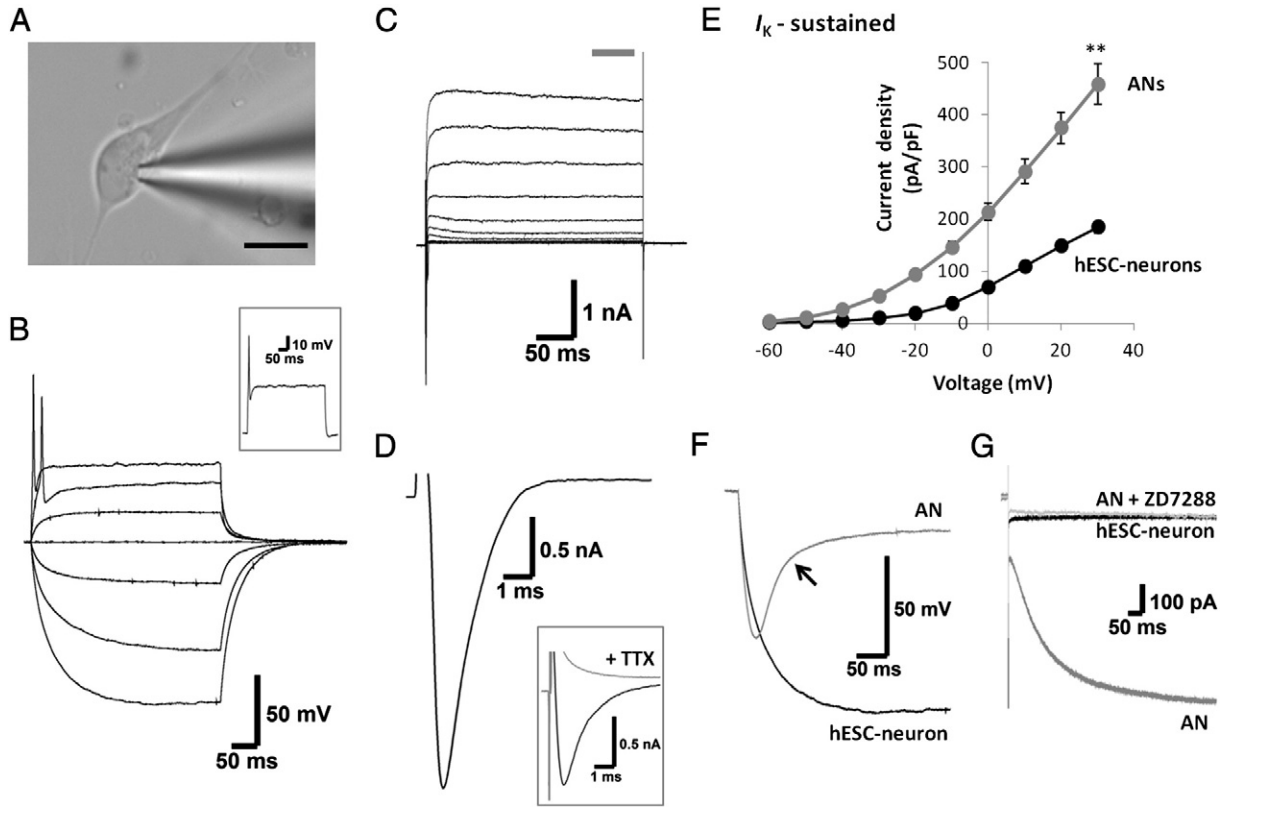

Figure 2 Electrophysiological properties of hESC-derived neurons. (A) A photomicrograph of a differentiated stem cell with bipolar morphology and recording electrode attached (scale bar — 10 μm). The typical profile observed in current-clamp (B) in response to current injections (−60 to 200 pA; holding potential of −73 mV) included a single action potential followed by a large, sustained depolarization during depolarizing current, and a large membrane hyperpolarization during hyperpolarizing current. Inset depicts activation of action potentials at the cell's resting membrane potential (−51 mV). In voltage-clamp (C–D), membrane depolarization evoked a fast inward sodium current (D) followed by a sustained outward K^+ current (C). Inset in D shows removal of the inward sodium current in the presence of 1 μM TTX (gray). A comparison with cultured primary auditory neurons (ANs; gray) revealed that the sustained portion of the outward K^+ current (I_K-sustained; measured over 50 ms period shown by bar in C) as displayed in current density (E), was smaller in stem cell-derived neurons (black). (F) Current-clamp recordings showed that hyperpolarization-evoked voltage 'sag' (denoted by arrow) observed in auditory neurons (gray) was absent in hESC-derived neurons (black). Likewise, in voltage-clamp recordings (G) stem cells (black) demonstrated a small inward current during hyperpolarization, whereas auditory neurons (gray) produced a large, slowly activating current that was abolished by the I_h-specific antagonist ZD7288 (light gray).

Results

Stem cell-derived neurons are physiologically active

Whole-cell patch clamp recordings were made from cells displaying a bipolar neuronal morphology (n = 86; Fig. 2A). The mean resting membrane potential (RMP) of the population was −49.2 ± 0.8 mV, while the mean input resistance (R_{IN}) was 1.4 ± 0.1 GΩ, and membrane capacitance was 7.7 ± 0.3 pF. This population of neurons did not display spontaneous firing, but were all capable of generating an action potential in response to membrane depolarization (Fig. 2B; examples shown for neurons at −73 mV holding potential or RMP [inset]). The majority of cells (68%) fired a single action potential at stimulus onset. Of the remaining cells, 26% fired a maximum of between 2 and 6 action potentials, and 6% displayed tonic firing (up to 13 action potentials). The mean maximum number of action potentials fired (AP_{Max}) across the population was 2.2 ± 0.2. Firing threshold was −39.3 ± 0.6 mV, with an average action potential amplitude of 91.6 ± 1.8 mV at threshold, or 100.3 ± 1.4 mV during supra-threshold input (+190 pA). The mean latency of action potentials was 40.2 ± 2.3 ms at threshold and 4.7 ± 0.2 ms with supra-threshold stimulation.

Voltage-clamp recordings were used to identify the key currents underlying the firing properties of stem cell-derived neurons. All cells examined in voltage-clamp displayed a fast-activating, rapidly inactivating inward current in response to increasing membrane depolarization (Figs. 2C–D). This transient inward current was abolished in the presence of 1 μM tetrodotoxin (TTX), a selective voltage-gated Na^+ channel antagonist (Fig. 2D inset). An I–V curve recorded in the presence of K^+ channel blockers 10 mM tetraethylammonium (TEA) and 1 mM 4-aminopyridine (4-AP) indicated that activation of I_{Na} occurred at potentials positive to −40 mV, with peak current at −13 mV (mean −106 ± 41 pA/pF; n = 4). To determine the voltage dependence of I_{Na}, normalized tail currents (measured at 0 mV following a −113 mV prepulse and voltage steps from −133 to −3 mV; data not shown) were fitted with a

Boltzmann function to reveal the mean half-activation voltage (V_h) of −55.4 ± 2.8 mV and slope factor (K) of 6.3 ± 1.1 (n = 4). The TTX-sensitive Na^+ current was followed by a sustained outward current (Fig. 2C), which could be attenuated by combined application of TEA and 4-AP as illustrated previously (Nayagam et al., 2013). The sustained portion of the outward current (denoted as I_K-sustained) increased steadily with increasing depolarization. When converted to current density (to account for possible variations in cell size), I_K-sustained was smaller than that observed in the population of primary auditory neurons (Fig. 2E). The difference between the populations was significant at +30 mV ($p < 0.001$; ANOVA).

In current-clamp, hyperpolarization of the cells evoked a steady change in membrane potential but did not evoke the classic voltage 'sag' response seen in primary auditory neurons (Fig. 2F). In addition, in voltage-clamp membrane hyperpolarization initiated a small, steady inward current (Fig. 2G). Unlike the primary auditory neurons, a large, slowly activating, non-inactivating inward current indicative of hyperpolarization-activated currents (I_h) was not observed (Fig. 2G). Instead, the current induced in hESCs closely matched that seen in auditory neurons in the presence of 50 μM ZD7288 (the I_h-selective antagonist), confirming the absence of the inward current mediated by hyperpolarization-activated cyclic nucleotide-gated (HCN) channels.

Firing properties with time in culture

The electrophysiological properties described to this point reflect the mean response across the entire population. To assess the stability or maturation of this response over time, firing properties were also considered relative to the period of time in culture. Recordings were made between 31 and 56 days *in vitro* (DIV), and grouped into the following clusters on the basis of mean time in culture; 31 DIV (n = 10), 35 DIV (n = 29), 42 DIV (n = 18), 48 DIV (n = 15), and 53 DIV (n = 14). Assessment of the passive membrane properties revealed no difference in RMP (Fig. 3A; $p = 0.28$; ANOVA), or change in R_{IN} with culture duration (Fig. 3B; $p = 0.23$; ANOVA). Firing threshold (Fig. 3C) was elevated at 35 DIV relative to the other time points, but this difference was only significant when compared to 48 DIV ($p = 0.004$; ANOVA). There was no significant difference in threshold between the other clusters, including between 31 DIV and 53 DIV. The maximum number of action potentials fired (AP_{Max}) showed increased variability after 31 DIV, with a significant change seen in mean AP_{Max} between groups (Fig. 3D; $p = 0.045$; ANOVA). Significant differences were evident between 31 DIV and 42 DIV ($p = 0.049$; t-test), 48 DIV ($p = 0.018$; t-test) and 53 DIV ($p = 0.028$; t-test). Firing latency at threshold (Fig. 3E) and in response to supra-threshold stimulation (Fig. 3G) were consistent with time in culture ($p = 0.29$ and $p = 0.34$ respectively; ANOVA). Further, no significant difference was seen in action potential amplitude (Fig. 3F; $p = 0.94$; ANOVA) or half-width (Fig. 3H; $p = 0.33$; ANOVA) measured during supra-threshold stimulation.

Firing entrainment to high frequency stimulation

To determine the ability of hESC-derived neurons to entrain to high frequency stimulation, firing activity was examined during a train of pulses. Supra-threshold pulses (1.0–2.0 nA; 0.3 ms duration) were presented from 2.5 to 1000 pulses per second (pps), and outcomes assessed as the probability of an action potential firing in response to each pulse (averaged

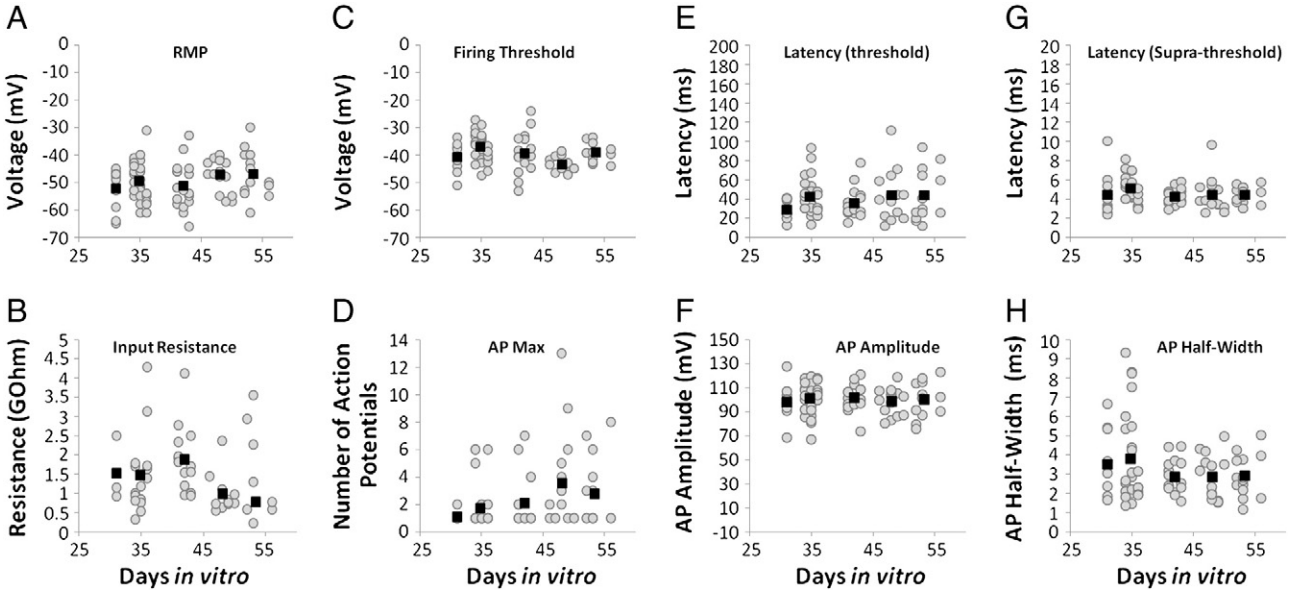

Figure 3 Firing properties of hESC-derived neurons with time in culture. The mean measure at each time point (black square) and individual responses (gray circles) are shown for resting membrane potential (RMP; A), input resistance (B), firing threshold (C), maximum number of action potentials fired during a 300 ms depolarization (D), latency of the first action potential (AP) at firing threshold (E) or supra-threshold (+190 pA; G), action potential amplitude (F), and action potential duration at 50% of its amplitude (half-width; H).

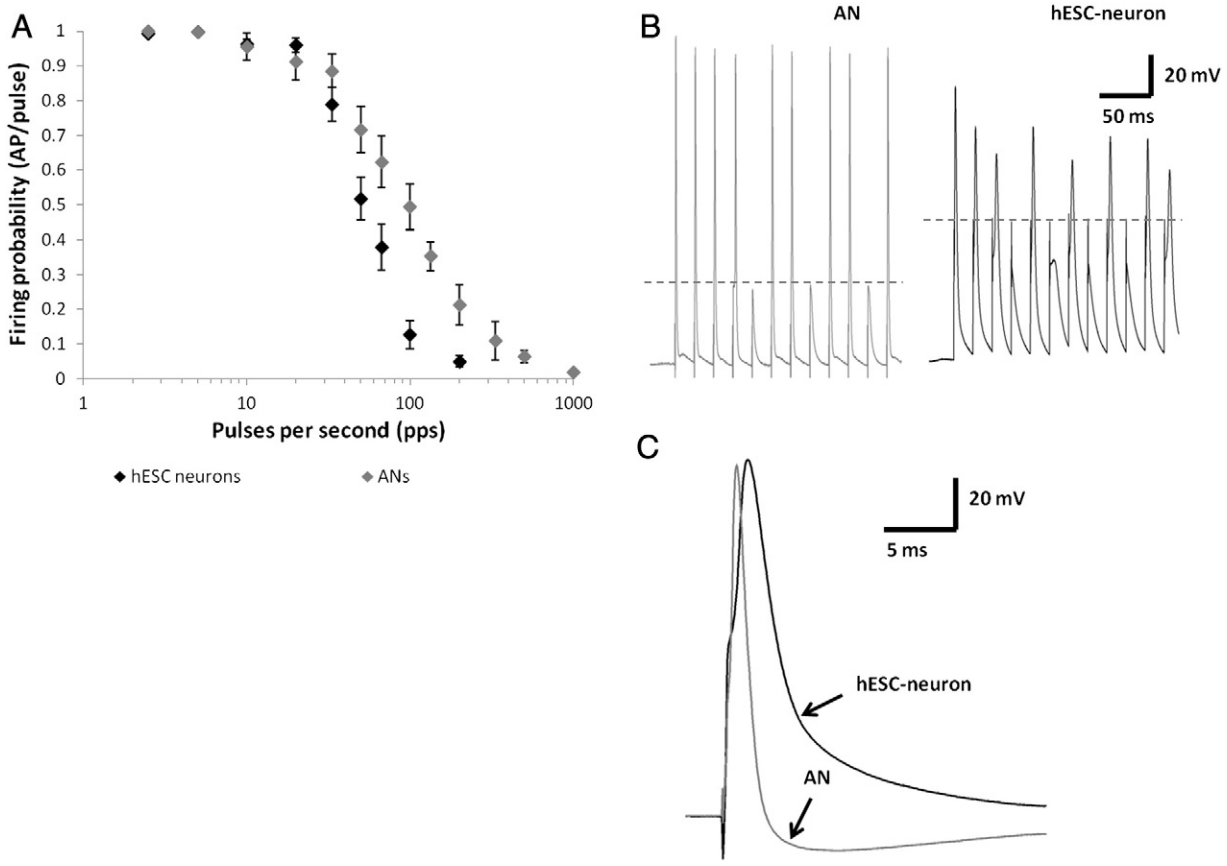

Figure 4 Firing activity in response to pulse trains. (A) Firing probability calculated as the number of action potentials fired per pulse, averaged over 50 presentations. The hESC neurons (black) did not entrain to stimuli as consistently as the primary auditory neurons (gray), as also shown by examples of firing responses during 67 pps stimuli (B) for a typical auditory neuron (AN; left) and hESC-neuron (right). Action potentials were distinguished from stimulus artifact as events >50 mV in amplitude; dashed lines illustrate relative amplitude of stimulus artifact in each example. (C) The longer latency and broader action potentials of the hESC-derived neurons (black) compared to auditory neurons (gray) contributed to their ability to reliably follow high frequency stimuli.

over a train of 50 pulses, and multiple presentations). As demonstrated in Fig. 4A, our population of stem cell-derived neurons (n = 43) displayed good firing entrainment (defined as a firing probability greater than 0.9) to stimuli presented between 2.5 and 20 pps. The probability fell to 0.5 at 50 pps (i.e. a 50% chance of firing to each pulse), and 0.05 by 200 pps. For comparison with the population of primary auditory neurons, we recorded firing activity of auditory neurons (n = 17) under the same conditions (Fig. 4A). While this population revealed a similar entrainment in response to stimuli presented from 2.5 to 20 pps, the reduction in firing probability with increasing stimulus rate was less pronounced. Instead, the reduction in firing entrainment to 0.5 was not observed until pulse trains of 100 pps. Firing probability was reduced to 0.06 at 500 pps, and 0.02 at 1000 pps. Differences between the groups were statistically significant at 67 pps (p = 0.025; ANOVA), 100 pps ($p < 0.001$; ANOVA) and 200 pps (p = 0.048; ANOVA).

Underlying the variance in firing entrainment between the stem cell-derived population and native auditory neurons was a significant difference in action potential latency and width (Figs. 4B–C). The latency of the first spike averaged 1.82 ± 0.15 ms in stem cell-derived neurons, as compared to 1.10 ± 0.09 ms in auditory neurons (p = 0.002; ANOVA), while half-width was 2.12 ± 0.11 ms in the stem cell population versus 0.93 ± 0.07 ms in auditory neurons ($p < 0.001$; ANOVA). Further, there were significant differences in the descending slope of the action potential ($p < 0.001$; hESC −27.37 ±2.23 mV/ms; auditory neurons −84.79 ± 9.57 mV/ms; ANOVA) and the time constant of the slow decay (p = 0.01; hESC 18.62 ± 2.51 ms; auditory neurons 6.32 ± 1.51 ms; ANOVA).

Discussion

This study describes the activity of human stem cell-derived neurons after extended time in culture, and in response to high frequency stimulation. The findings reported herein, confirm that our differentiation assay consistently produces a population of electrically active neurons which possess Na^+ and K^+ currents.

We have observed that the described population of stem cell-derived neurons predominantly displays a rapidly adapting phenotype. Classified in accordance with the previously defined convention for primary auditory neurons (Mo and Davis, 1997a; Adamson et al., 2002b), rapidly adapting cells fire between one and six action potentials during a 300 ms stimulus, while slowly adapting cells fire seven or more action potentials over the same period.

Interestingly, the predominance of this phenotype is comparable with recordings from early postnatal primary auditory neurons *in vitro*, where the majority displayed a rapidly adapting profile (Needham et al., 2012). In addition, murine stem cell-derived neurons uniformly show rapidly adapting responses over a period of 12 days *in vitro* (Tong et al., 2010). The rapidly adapting phenotype identified in the current study was stable for 5 weeks in culture, supporting the use of our excitable population of cells as replacement cells for auditory neurons.

The firing profile and physiological properties recorded from this population of stem cell-derived neurons nicely match those reported for embryonic day 14–15 (E14–15) mammalian auditory neurons *in situ* (Marrs and Spirou, 2012). In particular, both populations exhibit similar RMP, R_{IN}, and firing threshold, and display a broader action potential when compared to postnatal auditory neurons. Of additional interest is the absence of a voltage 'sag' in both E14–15 auditory neurons and our population of stem cell-derived neurons. The presence of a 'sag', and the hyperpolarization-activated current (I_h) which underlies this activity, is consistently reported in postnatal primary auditory neurons *in vitro* (Mo and Davis, 1997b; Szabo et al., 2002; Zhou et al., 2005; Needham et al., 2012), and has also been noted in later embryonic development of both primary auditory neurons and auditory brainstem neurons (Marrs and Spirou, 2012). This hints at I_h and voltage 'sag' as key markers of auditory neuron maturity. Notably, I_h, which regulates neuronal excitability in part through control of R_{IN}, can be influenced by the application of neurotrophins (Needham et al., 2012). Likewise, a lower (i.e. more hyperpolarized) RMP, which in our stem cell-derived neurons remained in the order of −50 mV across the 5 weeks *in vitro*, is also suggestive of a maturing neural phenotype and may also be assisted by the presence of BDNF in the culture media (Purcell et al., 2013). As recently demonstrated by Purcell et al. (2013), expression of the K^+ channel KCNQ4 dramatically increased in stem cell-derived neurons following BDNF exposure. These authors also reported a concomitant reduction in RMP, thereby highlighting the potential to produce specific neuronal subtypes using appropriate soluble molecules.

Physiological properties such as RMP and R_{IN} are of interest in terms of cochlear cell-based therapy, because these properties contribute to the overall responsiveness of replacement neurons to stimulation from a cochlear implant. Promisingly, our population of stem cell-derived neurons responded to low frequency pulsatile stimulation with high precision, however they were not able to match the efficiency of postnatal primary auditory neurons to entrain to high frequency input. Despite an extended period in culture, which we hypothesized may be sufficient to induce more electrically mature phenotypes, the present data suggest that other factors are required to reach this stage of maturation. Spontaneous activity and synapse formation are possible key steps in the production of mature electrical phenotypes from stem cell-derived neurons.

As indicated by the work of Marrs and Spirou (2012), one of the key factors in the maturation of auditory neurons is the formation of synapses with hair cells. Moreover, spontaneous firing may assist in directing the formation of specific synaptic connections and in activating auditory neurons during embryogenesis (Lippe, 1994). Spontaneous action potentials generated by immature inner hair cells are primarily mediated by Ca^{2+} channels, which disappear around the onset of hearing (Kros et al., 1998). The release of neurotransmitter at the basal surface of the inner hair cell is likely to modulate the activity of the developing auditory nerve (Beutner and Moser, 2001; Beutner et al., 2001). In a similar way, electrical stimulation has been shown to promote survival of auditory neurons *in vitro* (Hegarty et al., 1997; Hansen et al., 2001) and *in vivo* (Shepherd et al., 2005), and normal synaptic activity can be recovered following chronic electrical stimulation in congenitally deaf cats (Ryugo et al., 2005). Taken collectively, these data support the idea that spontaneous activity or electrical depolarization is an important feature in the terminal differentiation of auditory neurons, and this may be essential in order for them to reach their mature electrophysiological phenotype.

While the described population of stem cell-derived neurons was not observed to achieve a mature electrical phenotype *in vitro*, they may be capable of doing so once transplanted *in vivo*. Recent evidence suggests that stem cell-derived neurons can incorporate into the deaf gerbil cochleae, and improve auditory-evoked response thresholds after 10 weeks (Chen et al., 2012). Interestingly, the stem cell-derived neurons used by Chen et al. (2012) displayed similar basic firing properties prior to their transplantation, to the stem cell-derived neurons described in the present study. Moreover, the voltage-gated ion channels that control neural activity are sensitive to changes in their environment, including concentration of neurotrophic factors (Adamson et al., 2002a; Zhou et al., 2005; Needham et al., 2012; Purcell et al., 2013) and excitatory input (Leao et al., 2005; Holt et al., 2006; Hassfurth et al., 2009), both of which are likely to play a role following their transplantation into the deaf cochlea. Determining how to harness and balance both *in vitro* and *in vivo* factors to derive functionally appropriate stem cell-derived neurons will be an important task in developing a stem cell therapy for the deaf cochlea.

Acknowledgments

The authors thank Dr Clare L. Parish and Jessie Leung for technical laboratory support, and Marc L. Brady and John R. Brady for engineering support. This work has been supported by the National Health and Medical Research Council of Australia (Project Grant 1023372 and Fellowship 567117), The University of Melbourne, The Royal Victorian Eye and Ear Hospital, and Friedreich Ataxia Research Association. The funding bodies had no role in study design, data collection and analysis, decision to publish, or preparation of the manuscript.

References

Adamson, C.L., Reid, M.A., Davis, R.L., 2002a. Opposite actions of brain-derived neurotrophic factor and neurotrophin-3 on firing features and ion channel composition of murine spiral ganglion neurons. J. Neurosci. 22, 1385–1396.

Adamson, C.L., Reid, M.A., Mo, Z.L., Bowne-English, J., Davis, R.L., 2002b. Firing features and potassium channel content of murine spiral ganglion neurons vary with cochlear location. J. Comp. Neurol. 447, 331–350.

Beutner, D., Moser, T., 2001. The presynaptic function of mouse cochlear inner hair cells during development of hearing. J. Neurosci. 21, 4593–4599.

Beutner, D., Voets, T., Neher, E., Moser, T., 2001. Calcium dependence of exocytosis and endocytosis at the cochlear inner hair cell afferent synapse. Neuron 29, 681–690.

Brown, W.G.A., Needham, K., Nayagam, B.A., Stoddart, P.R., 2013. Whole cell patch clamp for investigating the mechanisms of infrared neural stimulation. J. Vis. Exp. (77), e50444. http://dx.doi.org/10.3791/50444.

Chen, W., Johnson, S.L., Marcotti, W., Andrews, P.W., Moore, H.D., Rivolta, M.N., 2009. Human fetal auditory stem cells can be expanded in vitro and differentiate into functional auditory neurons and hair cell-like cells. Stem Cells 27, 1196–1204.

Chen, W., Jongkamonwiwat, N., Abbas, L., Eshtan, S.J., Johnson, S.L., Kuhn, S., Milo, M., Thurlow, J.K., Andrews, P.W., Marcotti, W., Moore, H.D., Rivolta, M.N., 2012. Restoration of auditory evoked responses by human ES-cell-derived otic progenitors. Nature 490, 278–282.

Denham, M., Dottori, M., 2011. Neural differentiation of induced pluripotent stem cells. Methods Mol. Biol. 793, 99–110.

Dottori, M., Pera, M., 2008. Isolation and culture of NSCs. In: Weiner, L.P. (Ed.), Neural Stem Cells: Methods and Protocols. Humana Press, Totowa, pp. 19–30.

Gunewardene, N., Dottori, M., Nayagam, B.A., 2012. The convergence of cochlear implantation with induced pluripotent stem cell therapy. Stem Cell Rev. 8, 741–754.

Gunewardene, N., Needham, K., Dottori, M., Nayagam, B.A., 2013. The potential of induced pluripotent stem cells for auditory neuron replacement. Proceedings of the Australian Neuroscience Society, Melbourne, p. 73.

Hansen, M.R., Zha, X.M., Bok, J., Green, S.H., 2001. Multiple distinct signal pathways, including an autocrine neurotrophic mechanism, contribute to the survival-promoting effect of depolarization on spiral ganglion neurons in vitro. J. Neurosci. 21, 2256–2267.

Hassfurth, B., Magnusson, A.K., Grothe, B., Koch, U., 2009. Sensory deprivation regulates the development of the hyperpolarization-activated current in auditory brainstem neurons. Eur. J. Neurosci. 30, 1227–1238.

Hegarty, J.L., Kay, A.R., Green, S.H., 1997. Trophic support of cultured spiral ganglion neurons by depolarization exceeds and is additive with that by neurotrophins or cAMP and requires elevation of [Ca2+]i within a set range. J. Neurosci. 17, 1959–1970.

Holt, A.G., Asako, M., Duncan, R.K., Lomax, C.A., Juiz, J.M., Altschuler, R.A., 2006. Deafness associated changes in expression of two-pore domain potassium channels in the rat cochlear nucleus. Hear. Res. 216–217, 146–153.

Hotta, R., Pepdjonovic, L., Anderson, R.B., Zhang, D., Bergner, A.J., Leung, J., Pebay, A., Young, H.M., Newgreen, D.F., Dottori, M., 2009. Small-molecule induction of neural crest-like cells derived from human neural progenitors. Stem Cells 27, 2896–2905.

Huisman, M.A., Rivolta, M.N., 2012. Neural crest stem cells and their potential application in a therapy for deafness. Front. Biosci. (Schol. Ed.) 4, 121–132.

Javel, E., Viemeister, N.F., 2000. Stochastic properties of cat auditory nerve responses to electric and acoustic stimuli and application to intensity discrimination. J. Acoust. Soc. Am. 107, 908–921.

Kiang, N.Y., Pfeiffer, R.R., Warr, W.B., Backus, A.S.N., 1965. Stimulus coding in the cochlear nucleus. Ann. Otol. Rhinol. Laryngol. 74, 463–485.

Kros, C.J., Ruppersberg, J.P., Rusch, A., 1998. Expression of a potassium current in inner hair cells during development of hearing in mice. Nature 394, 281–284.

Leao, R.N., Svahn, K., Berntson, A., Walmsley, B., 2005. Hyperpolarization-activated (*I*) currents in auditory brainstem neurons of normal and congenitally deaf mice. Eur. J. Neurosci. 22, 147–157.

Lippe, W.R., 1994. Rhythmic spontaneous activity in the developing avian auditory system. J. Neurosci. 14, 1486–1495.

Liu, J., Sumer, H., Leung, J., Upton, K., Dottori, M., Pebay, A., Verma, P.J., 2011. Late passage human fibroblasts induced to pluripotency are capable of directed neuronal differentiation. Cell Transplant. 20, 193–203.

Livak, K.J., Schmittgen, T.D., 2001. Analysis of relative gene expression data using real-time quantitative PCR and the 2(−Delta Delta *C*(*T*)) Method. Methods 25 (4), 402–408.

Marrs, G.S., Spirou, G.A., 2012. Embryonic assembly of auditory circuits: spiral ganglion and brainstem. J. Physiol. 590, 2391–2408.

Mo, Z.L., Davis, R.L., 1997a. Endogenous firing patterns of murine spiral ganglion neurons. J. Neurophysiol. 77, 1294–1305.

Mo, Z.L., Davis, R.L., 1997b. Heterogeneous voltage dependence of inward rectifier currents in spiral ganglion neurons. J. Neurophysiol. 78, 3019–3027.

Nayagam, B.A., Edge, A.S., Needham, K., Hyakumura, T., Leung, J., Nayagam, D.A., Dottori, M., 2013. An in vitro model of developmental synaptogenesis using cocultures of human neural progenitors and cochlear explants. Stem Cells Dev. 22, 901–912.

Needham, K., Nayagam, B.A., Minter, R.L., O'Leary, S.J., 2012. Combined application of brain-derived neurotrophic factor and neurotrophin-3 and its impact on spiral ganglion neuron firing properties and hyperpolarization-activated currents. Hear. Res. 291, 1–14.

Needham, K., Minter, R.L., Shepherd, R.K., Nayagam, B.A., 2013. Challenges for stem cells to functionally repair the damaged auditory nerve. Expert. Opin. Biol. Ther. 13, 85–101.

Purcell, E.K., Yang, A., Liu, L., Velkey, J.M., Morales, M.M., Duncan, R.K., 2013. BDNF profoundly and specifically increases KCNQ4 expression in neurons derived from embryonic stem cells. Stem Cell Res. 10, 29–35.

Ryugo, D.K., Kretzmer, E.A., Niparko, J.K., 2005. Restoration of auditory nerve synapses in cats by cochlear implants. Science 310, 1490–1492.

Seligman, P., Shepherd, R.K., 2004. Cochlear implants. In: Horch, K.W., Dhillon, G.S. (Eds.), Neuroprosthetics: Theory and Practice. World Scientific Press, Singapore, pp. 878–904.

Shannon, R.V., 1983. Multichannel electrical stimulation of the auditory nerve in man. I. Basic psychophysics. Hear. Res. 11, 157–189.

Shepherd, R.K., Coco, A., Epp, S.B., Crook, J.M., 2005. Chronic depolarization enhances the trophic effects of brain-derived neurotrophic factor in rescuing auditory neurons following a sensorineural hearing loss. J. Comp. Neurol. 486, 145–158.

Shi, F., Corrales, C.E., Liberman, M.C., Edge, A.S., 2007. BMP4 induction of sensory neurons from human embryonic stem cells and reinnervation of sensory epithelium. Eur. J. Neurosci. 26, 3016–3023.

Szabo, Z.S., Harasztosi, C.S., Sziklai, I., Szucs, G., Rusznak, Z., 2002. Ionic currents determining the membrane characteristics of type I spiral ganglion neurons of the guinea pig. Eur. J. Neurosci. 16, 1887–1895.

Tong, M., Hernandez, J.L., Purcell, E.K., Altschuler, R.A., Duncan, R.K., 2010. The intrinsic electrophysiological properties of neurons derived from mouse embryonic stem cells overexpressing neurogenin-1. Am. J. Physiol. Cell Physiol. 299, C1335–C1344.

Vandali, A., Sly, D., Cowan, R., van Hoesel, R., 2013. Pitch and loudness matching of unmodulated and modulated stimuli in cochlear implantees. Hear. Res. 302, 32–49.

Yang, R., Xu, X., 2013. Isolation and culture of neural crest stem cells from human hair follicles. J. Vis. Exp. (74), e3194. http://dx.doi.org/10.3791/3194.

Zeng, F.G., 2002. Temporal pitch in electric hearing. Hear. Res. 174, 101–106.

Zhou, Z., Liu, Q., Davis, R.L., 2005. Complex regulation of spiral ganglion neuron firing patterns by neurotrophin-3. J. Neurosci. 25, 7558–7566.